pubs.acs.org/jasms Research Article

Effect of Jitter on Digital Mass Filter Analysis in Higher Stability Zones

Sumeet Chakravorty, Fatima Olayemi Obe, Elizabeth Groetsema, and Peter T. A. Reilly*



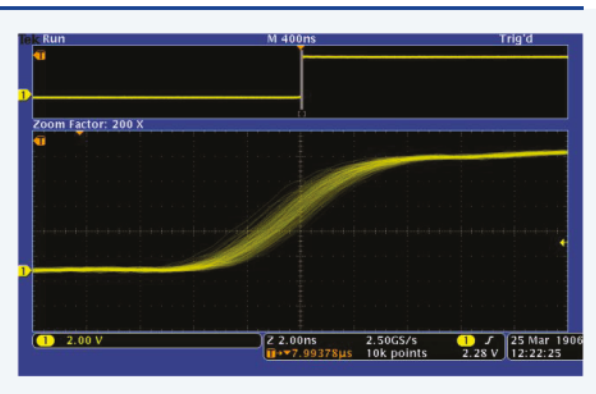
Cite This: https://doi.org/10.1021/jasms.2c00293



ACCESS |

Metrics & More

ABSTRACT: Waveform reproducibility is a critical factor for performing high resolution mass analysis with digitally operated quadrupole mass filters and traps operating in higher stability zones. In this work, Hill equation-based stability calculations were used to define the effect of period jitter on mass analysis in higher stability zones. These calculations correlate well with experimental observations in higher stability zones. Comparison of experiment to theory supplies the basis for defining jitter-based expectations and limits for mass analysis in higher zones.



Article Recommendations

■ INTRODUCTION

The reproducibility of rectangular waveforms on a wave-towave basis is determined by measuring the variation in the waveform period (ΔT) with an oscilloscope divided by the period of the waveform $(\Delta T/T)$. This is done using the delay feature and triggering off the leading edge of one wave and zooming into the leading edge of the next. This measurement is demonstrated in Figure 1 at 100 kHz. The waveform's

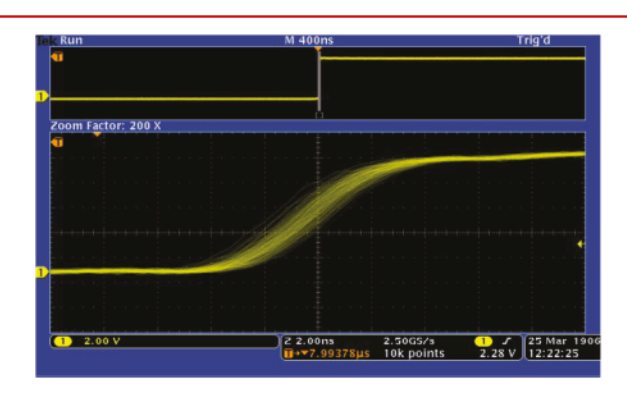


Figure 1. Period jitter measurement (2 ns) at 100 kHz for the Comparator-based WFG.

period varies randomly by roughly ± 1 ns around the average of 10.000 μ s and has a normal distribution. The cycle-to-cycle period jitter (ΔT) is defined as the width of the variation ~ 2 ns.

The Hill equation can be used to define the effect of the jittering waveform period because it is used to calculate ion

stability in Mathieu (a, q) space within a digital mass filter (DMF) over one waveform period. Normally, this calculation assumes the reproducibility of the periodic waveform. 1-3 However, stability in Mathieu space can be translated into the laboratory frame as the pseudopotential well depth.^{4,5} Then, the Mathieu parameters a and q can be used to plot the pseudopotential as a function of m/z by specifying the radius, voltage, and frequency. An example of the pseudopotential well depth versus m/z for zone 3,1 at q = 4.5, a = 0, $r_0 = 4.17$ mm, V= 100 V_{0-p}, and 100 kHz is shown in Figure 2. This pseudopotential well is defined at precisely 100,000 Hz or T =10.0000 μ s. Jitter of ± 1 ns causes the frequency to fluctuate around 100,000 Hz (blue well) between 99,990 (gray well) and 100,010 Hz (orange well) (see Figure 3a). In this case, the pseudopotential well can be thought of as randomly "jumping" around or jittering between these frequency limits from one cycle to the next. Figure 3a defines the period jitter-induced spread of the mass wells.

The duty cycle is also jittering. Changes in the duty cycle shifts the axial wells along the mass axis and thereby shifts the stability well. ^{5,6} The magnitude of these duty cycle based jitter shifts yield similar fractional well overlap in comparison to period jitter. The two forms of jitter cannot be experimentally

Received: October 12, 2022 Revised: November 19, 2022 Accepted: November 23, 2022



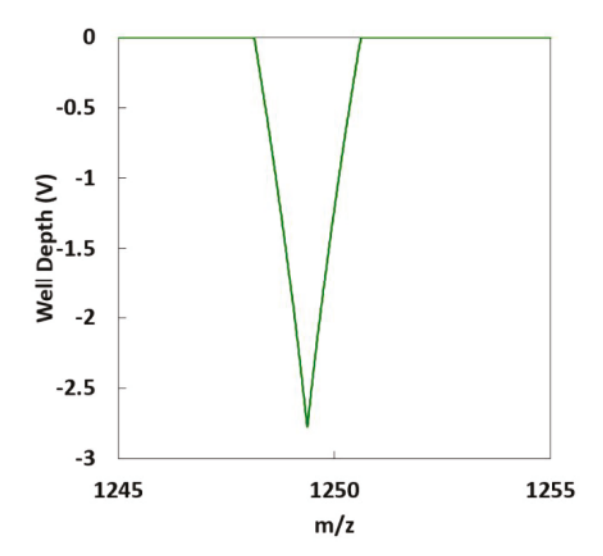


Figure 2. Zone 3,1 pseudopotential mass well at a = 0, $r_0 = 4.17$ mm, V = 100 V, and 100,000 Hz.

separated. The effects of these two types of jitter get lumped together because you cannot have one without the other in roughly equal proportion and so we only use period jitter to refer to both types of jitter and perform the evaluation.

The fractional overlap between the jittering wells is defined by the clear area at the center bound by the orange well on the high mass side and the gray well on the low side. Because the blue well and the overlap are similar triangles, the fractional overlap is defined by the square of the ratio of overlap well depth (define by the intersection of the orang and gray wells at 2.1 V) to the blue well depth 2.8 V, $2.1^2/2.8^2 = 0.56$. This fractional overlap definition will be used to evaluate period jitter-based transmission reduction.

Each jittering waveform experienced by the ions results in a change in pseudopotential well depth for a precise value of m/z. Even when the well jitters around the ion mass so that the well depth is always negative with each cycle, the well depth changes yield radial excitation with each cycle. When the well jitters outside of the ion mass so that the ion mass is not within the negative well for some of the cycles, the rate of excitation increases exponentially the farther the ion mass is from the well. The ability of the ions to pass through the mass filter depends on the amount of excitation they receive as they transmit and the average amount of excitation they achieve depends on the dispersion of the jitter mass wells and the number of jittering waveforms experienced by the ion during transit (i.e., beam energy).

Jitter or temporal resolution (ΔT) is often assumed to be random and constant with frequency. If true, the waveform reproducibility ($\Delta T/T$) decreases with increasing frequency or decreasing mass. To demonstrate the effect of constant jitter with frequency over the typical range of a mass scan, the range of well depth jitter at 500 kHz under the same conditions as Figure 3a is shown in Figure 3b. A \pm 1 ns jitter at 500,000 Hz yields frequencies that range from 499,750 (gray well) to 500,250 Hz (orange well). The blue wells in (a) and (b) represent the wells at the ion mass around which the mass wells jitter. Comparison of (a) and (b) shows that the jitter induced mass well overlap gets worse with increasing frequency or decreasing m/z. Better jitter well overlap yields

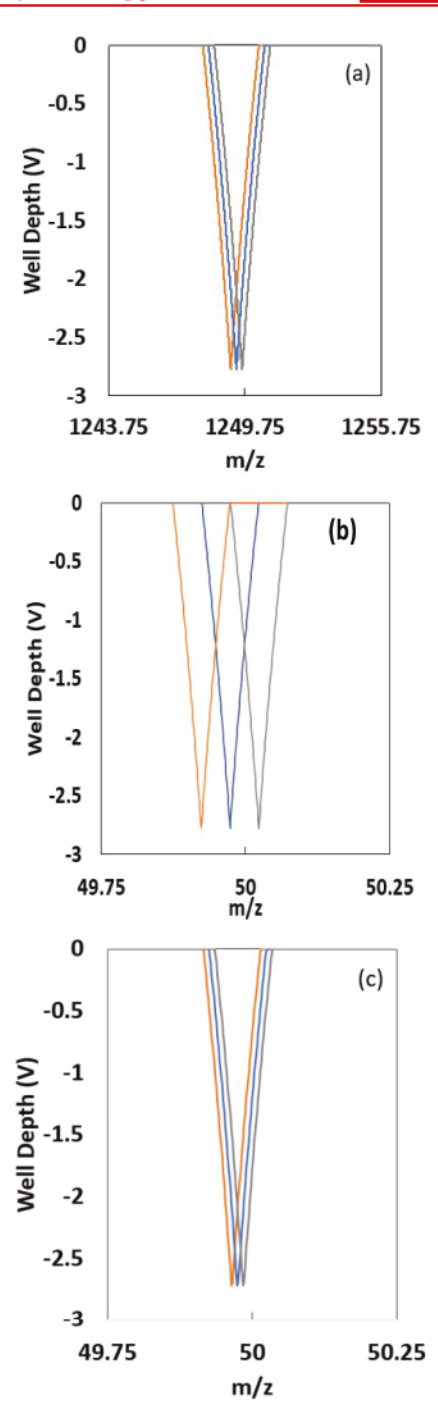


Figure 3. Zone 3,1 jitter-based mass well spread (a) at 100 kHz \pm 1 ns jitter, (b) at 500 kHz \pm 1 ns jitter, and (c) at 500 kHz and \pm 200 ps jitter. The jitter spread of (a) and (c) are the same at constant temporal precision when $T/\Delta T=$ constant.

better ion transmission. Consequently, jitter has less of an effect at higher m/z—assuming the period jitter is constant.

The constant jitter concept requires the jitter to be purely random without any part of the generation system affecting it. The comparison method for generating rectangular waveforms systematically generates jitter during the triggering of the comparator. In this case, triggering jitter depends on the temporal slope of the waveform at the comparison voltage. DDS generated triangular waves were chosen over sine waves to keep the temporal jitter constant as a function of duty cycle

in the hope that mass analysis at higher duty cycle could be achieved. The slopes of triangular waves are linear with respect to the waveform period T and so the period over which the comparator can switch ΔT also changes linearly with T. This means that the waveform reproducibility is constant with frequency. This idea was corroborated by measuring the waveform jitter from our comparator-based waveform generator that uses DDS generated triangular waves at 500 kHz with the oscilloscope to be 0.40 ns, a factor of 5 smaller than the 2 ns jitter measured at 100 kHz. The effect of constant jitter-based precision on the mass well jitter at 500 kHz is shown in Figure 3c where the frequency jitters between 499,950 and 500,050 Hz around 500,000 Hz.

Analysis of Figure 3 shows that, in the case of constant jitter with respect to frequency, the dispersion of the jitter wells gets smaller with increasing m/z (compare Figure 3a and b). Figure 3 further suggests that constant waveform reproducibility $(\Delta T/T = \text{constant})$ yields less of an effect on the dispersion of the jittering wells (i.e., their percent overlap) and does not change with frequency. However, that notion assumes that the waveform period jitter ΔT is proportional to the period T and that the comparator generated jitter is greater than the omnipresent random jitter that arises from components such as the system clock, DDS, FPGAs, or digital counters. Consequently, the random constant jitter from these components is generally significantly smaller than the jitter that results from waveform comparison.

Our calculation results suggest that the best achievable resolving power will be observed when there is no jitter (i.e., no mass well dispersion) and then the theoretical resolving power will be achieved. Jitter broadens the baseline transmissible mass window while reducing the transmitted ion flux. Consequently, the effect of jitter on the higher stability zones can be determined by comparing the experimentally measured resolving powers with the theoretical values and the transmitted ion intensity.

■ EXPERIMENTAL SECTION

The jitter measurements were made on a Rigol 350 MHz oscilloscope with a 4 GHz sampling rate. The measurements were also made with a 300 MHz Tektronix oscilloscope with 2.5 GHz sampling rate and yielded the same results.

Calculations of the pseudopotential well depth were made using matrix solutions of the Hill equation. These calculations were performed using a spreadsheet program entitled "m/z vs pseudopotential well depth plot" that can be found on our group website, https://reilly.chem.wsu.edu/spreadsheet-stability-programs/. It is available to the public for download.

Digital mass filter analysis was performed using an electron impact ionization (EI) source followed by an eight-inch-long SCIEX analyzing quadrupole and electron multiplier detector in a separate chamber at 1×10^{-5} Torr. The mass filter was operated with rectangular waveforms produced from a digital waveform generator (WFG) that consists of a digital WFG⁸ invented by our group that produces low voltage rectangular waves with 10 ppm duty cycle resolution. The low voltage rectangular waves were used to gate commercial high voltage pulsers (Directed Energy Inc., PVX-4150, https://directedenergy.com/product/pvx-4150/) to create the high voltage digital waveforms. Operations in the higher stability zones were performed with parameters (i.e., duty cycle, well depth, q-value, etc.) defined in ref 9. All analyses were

performed with perfluorotributyl amine (PFTBA) purchased from Scientific Instrument Services Inc. (Ringoes, NJ).

COMPARISON OF EXPERIMENTAL AND THEORETICAL RESULTS

Zone 2,1 has been chosen for the first comparison of the jittering mass wells with the experimentally obtained results from the electron impact (EI) spectrum of PFTBA. Figure 4a

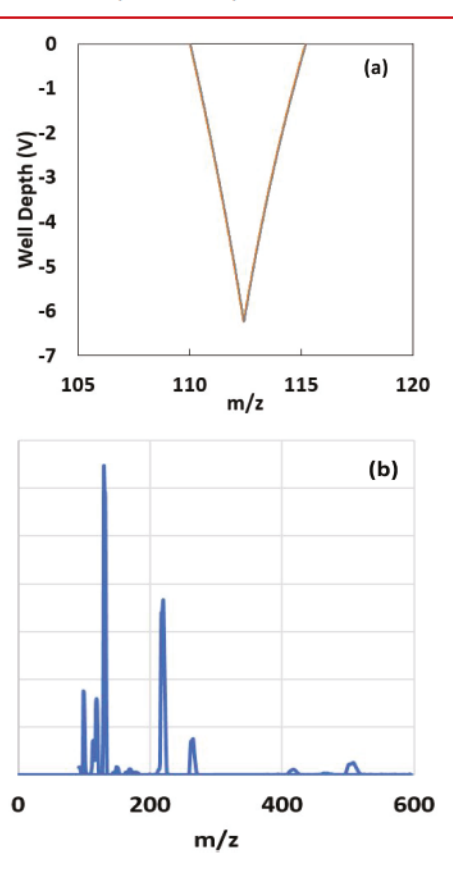


Figure 4. Zone 2,1 (a) jitter well depth vs m/z plots at 100 V_{0-p}, at 500 kHz with ± 1 ns jitter at 499,990, 500,000, and 500,010 Hz. Theoretical RP_{BL} = 22, RP_{1/2} = 50. (b) PFTBA EI spectrum, 5 V beam energy, RP_{BL} = 22, RP_{1/2} = 45 for m/z 131, S/N = 1500. The spectrum was not averaged.

shows plots of the well depth versus m/z at 500 kHz and at the ±200 ps jitter extremes at frequencies 499,950 (gray), 500,000 (blue), and 500,050 Hz (orange). These values were chosen because our comparison-based waveform generator (WFG) was used in the experiment that has a measured jitter at 400 ps at 500 kHz. These jitter wells completely overlap each other at ±200 ps jitter and 500 kHz. Their fractional overlap is 1.00. The fact that the 100 ppm waveform precision does not change with frequency suggests that this level of precision does not affect zone 2,1 ion transmission. Our EI spectra with PFTBA in Figure 4b corroborate this idea because the ion transmission is intense (S/N = 1500) and the measured resolving powers match the theory very closely over the range of the spectrum. This suggests that waveform precision $(\Delta T/T)$ defines the resolving power and transmission. In the case of zone 2,1, the primary reason for the alignment of theory and experiment is that the baseline resolving power of zone 2,1 is low $RP_{BL} = 22$ relative to the magnitude of the 100 ppm waveform precision. As the resolving power increases so too will the effect of jitter

to the detriment of transmission and achievable resolving power. This theory/experiment comparison provides a high transmission benchmark that can be used to determine the effect of jitter (i.e., waveform precision) on performance in other stability zones.

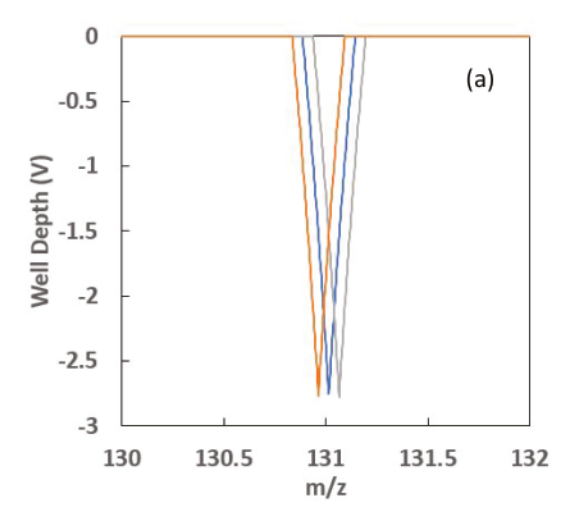
The higher zones provide better resolution and so they are expected to be affected by jitter to a greater extent. Our group has made DMF measurements in zones 3,1 and 3,2. Zone 3,1 has a theoretical resolving power of RP_{BL} = 511 and RP_{1/2} = 1113. DMF measurements were performed with PFTBA at 100 V_{0-p} on the m/z 131 peak from the EI spectrum. The jitter mass well spread was calculated for our comparator-based WFG at m/z 131 around the frequency of 308.8 kHz. Since the jitter base waveform reproducibility $\Delta T/T$ is constant at 100 ppm for our WFG, the jitter at 308,800 Hz can be calculated by ratio from eq 1:

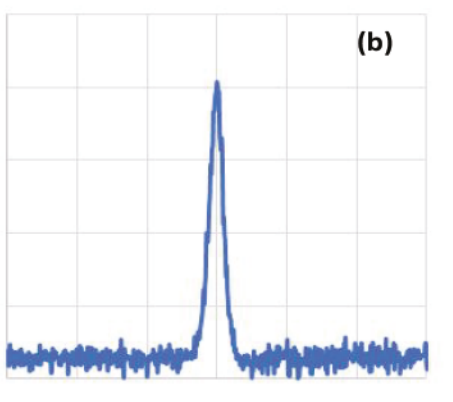
$$\frac{T_2}{\Delta T_2} = \frac{T_1}{\Delta T_1}, \quad \Delta T_2 = \frac{T_2}{T_1} \Delta T_1 = \frac{F_1}{F_2} \Delta T_1$$
 (1)

The jitter limits of the mass wells were then calculated at ± 324 ps with frequencies that range between 308,769 and 308,831 and the center at 308,800 Hz. The mass wells are depicted in Figure 5a. There is a 0.29 overlap between the jittering wells that indicates ion transmission can be achieved. DMF analysis in zone 3,1 required significant ion beam energy to observe and optimize the ion signal. Figure 5b shows the m/z 131 peak from zone 3,1 at 30 V beam energy. The measured resolving powers of the m/z 131 peak from zone 3,1 were RP_{BL} = 300 and RP_{1/2} = 670, while the signal-to-noise ratio (S/N) was \sim 20.

The same procedure was used to evaluate zone 3,2 at m/z131 in Figure 6. The jiter mass well spread is shown in Figure 6a with a fractional overlap of 0.13. At 100 V_{0-p} , m/z 131 has a frequency of 231,613 Hz with ± 432 ps jitter. The jittering wells were calculated at 231,590 (gray), 231,613 (blue), and 231,636 Hz (orange). The spread of the zone 3,2 wells is greater than the zone 3,1 wells relative to their baseline width. The poor fractional overlap suggests that a lower S/N than observed in Figure 4b and a lower resolving power relative to the theoretical value will be attained. Additionally, a greater beam energy should be required to obtain transmission. Indeed, these characteristics were observed with a measured S/ $N = \sim 9$ attained at 75 V beam energy. Although the obtained resolving powers were greater than zone 3,1 at $RP_{BL} = 500$ and $RP_{1/2}$ = 1200, they are significantly lower than the theoretical values at 1511 and 3425. When compared as percentages, zone 3,2 resolving powers were about 33% of the theoretical values whereas zone 3,1 was about 60%. This result appears to correlate with the change in fractional jitter well overlap (compare Figures 5a and 6a). In the case of zone 2,1 the overlap is nearly perfect and the experimental and theoretical values are roughly the same (see Figure 4a).

The changes in S/N between zones 2,1, 3,1, and 3,2 are harder to understand. If zone 2,1 sets the standard for high transmission in the higher zones purely because the jitter mass wells almost completely overlap, then the factor of ~75 reduction in S/N between zones 2,1 and 3,1 given the relatively small change of jitter well overlap does not explain the change in transmission. The disparity likely arises because the characteristics exhibited by jitter can also be attributed to acceptance. Acceptance decreases ion transmission by rapid ion excitation in the unstable fringe regions, whereas jitter





128 129 130 131 132 133 134 m/z

Figure 5. Zone 3,1 (a) jitter well depth vs m/z plots at $100~\rm V_{0-p}$, at $308.8~\rm kHz$ with $\pm 309~\rm ps$ jitter at 308,770, 308,800, and $308,830~\rm Hz$. Theoretical $\rm RP_{BL}=511$, $\rm RP_{1/2}=1,113$. (b) PFTBA EI spectrum, $30~\rm V$ beam energy, $\rm RP_{BL}=300$, $\rm RP_{1/2}=670~\rm for~m/z~131$, $\rm S/N=\sim 20$. The spectrum was averaged $10~\rm times$.

causes radial excitation in the stable region of the DMF where the fields are fully developed. Additionally, the acceptance is known to decrease as the resolving power increases.

In continuous ion transmission mode, it is not possible to separate the effects of acceptance and jitter. For both phenomena, a higher transmission is achieved at a higher beam energy or fewer waveform cycles experienced during transmission through the fields. In general, fewer waveform cycles also yield lower resolution. Jitter during transmission through the fully developed fields induces radial excitation with every cycle because the well depth changes with each cycle.7 Inside evacuated mass filters, there is no mechanism for reduction of radial excitation; therefore, the ions continuously excite as they pass through the fields. When the ions attain enough excitation, they radially eject. Transmission into and through the filter depends on the rate and the duration of excitation in the fringe and fully developed fields. The rate of excitation depends on the spread of the jittering wells and the resolving power of the zone. Higher zones yield higher resolution and rates of excitation, they require fewer cycles to separate unstable and stable ions, and they are correspondingly

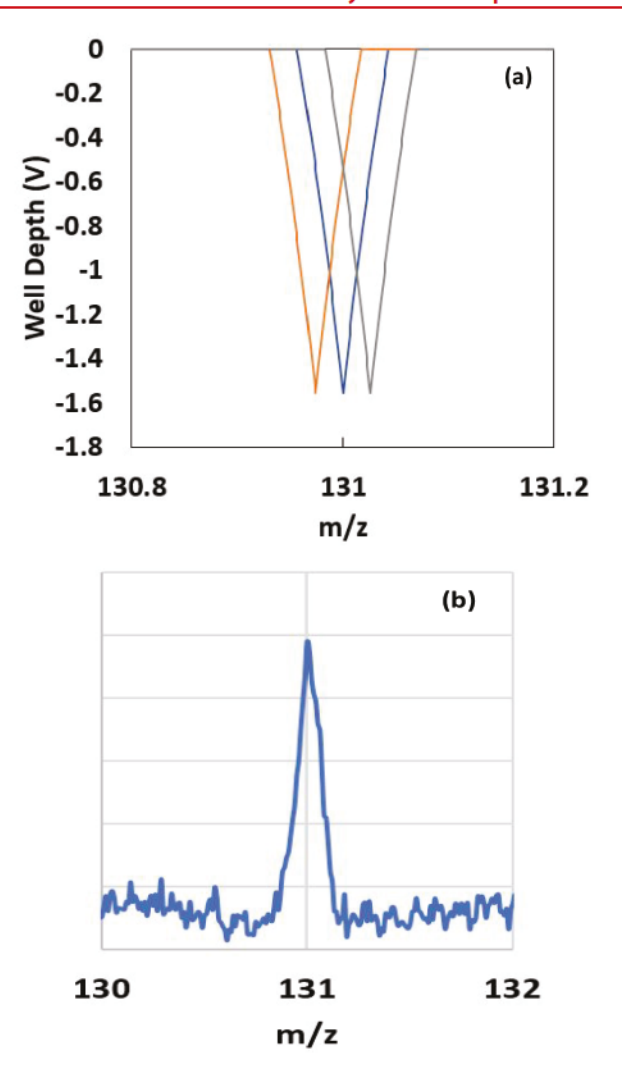


Figure 6. Zone 3,2 (a) jitter well depth vs m/z plots at 100 V_{0-p}, at 231.6 kHz with ± 432 ps jitter at 231,590, 231,613, and 231636 Hz. Theoretical RP_{BL} = 1,511, RP_{1/2} = 3,425. (b) PFTBA EI spectrum, 75 V beam energy, RP_{BL} = 500, RP_{1/2} = 1,200 for m/z 131, S/N = \sim 9. The spectrum was averaged 10 times.

more susceptible to jitter and acceptance. While jitter reduces transmission, it also increases the m/z range of ions that can be transmitted through the filter. It allows ions that would normally be outside the transmission mass window to enter the filter and transmit with some probability that diminishes as the

mass difference increases. Consequently, reduction in resolving power, signal-to-noise ratio, and required increase in ion beam energy are characteristic of not only jitter but also acceptance.

PROJECTING WAVEFORM REPRODUCIBILITY REQUIREMENTS FOR HIGHER STABILITY ZONES

The jitter well calculation can be used to project the required waveform reproducibility to obtain the theoretical limit of the resolving power in each of the stability zones. The jitter well calculation performed in Figure 3a for zone 3,1 at 100 kHz is reproduce in Figure 7a with a factor of 10 reduction in jitter. Jitter of ± 100 ps causes the frequency to fluctuate around 100,000 Hz (blue well) between 99,999 (gray well) and 100,001 Hz (orange well). These jitter wells have a fractional overlap of 1.00 at m/z 1249 and so 10 ppm waveform reproducibility should provide the theoretical limits for resolving power for zone 3,1.

In comparison to zone 3,1, zone 3,2 has a theoretical resolving power that is roughly a factor of 3 greater ($RP_{1/2} = 3,425$). So, while, \pm 100 ps jitter at 100 kHz yields unit fractional jitter well overlap for zone 3,1, the overlap is 0.76 for zone 3,2 (see Figure 7b). Consequently, the experimental resolving power should only approach the theoretical value at 10 ppm reproducibility. However, improving the reproducibility by another factor of 10 to 1 ppm (10 ps at 100 kHz) as shown in Figure 7c will yield unit fractional overlap and the theoretical resolving power values should be achieved.

Zone 4,1 has an $\mathrm{RP}_{1/2}=28,572$, which is almost an order of magnitude greater than zone 3,2. Consequently, zone 4,1 at 10 ps at 100 kHz (1 ppm reproducibility) yields significant mass well dispersion with a fractional overlap of 0.67. This jitter well plot is shown in Figure 8a. It is similar to Figure 7b and suggests it will fall short of the theoretical values. High resolution in zone 4,1 requires the waveform reproducibility to improve by another factor of 10 to 0.1 ppm (1 ps at 100 kHz) to obtain complete overlap like Figure 7 c.

Figure 8 evaluates the reproducibility requirements to observe zones 4,2 and 5,1 at 100 kHz. These zones operate at the same q value, 12.50, and they center at the same m/z 449.756. The theoretical resolving powers are $RP_{1/2}=79$ and 616 k, respectively. There is roughly an order of magnitude increase in resolving power. The zone 4,2 jitter wells shown in Figure 8a were calculated at 99,999.9 (gray), 100,000.0 (blue), and 100,000.1 Hz (orange) with ± 10 ps jitter (1 ppm reproducibility). They yield a fractional overlap of 0.67. The zone 5,1 jitter wells are shown in Figure 8b. They were

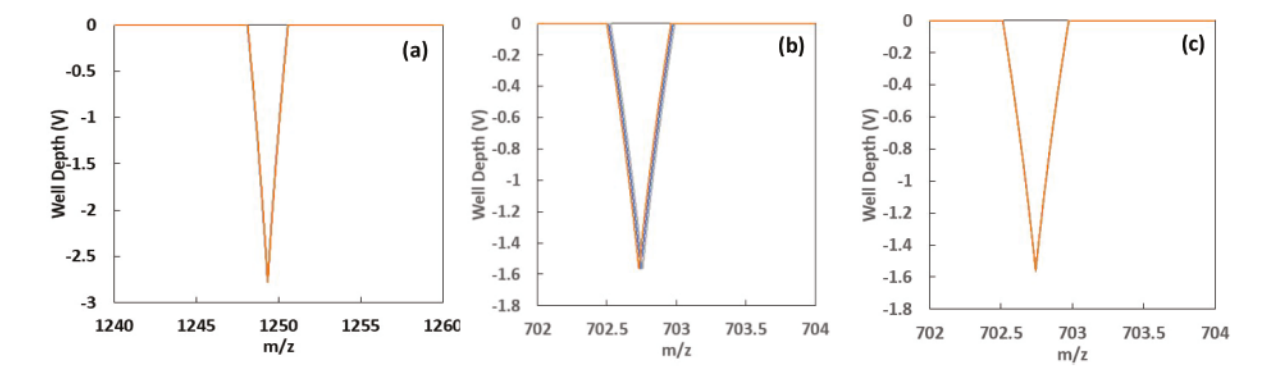


Figure 7. Jitter well spread calculation of (a) zone 3,1 ($RP_{1/2} = 1113$) at 100 kHz with ± 100 ps jitter, (b) zone 3,2 ($RP_{1/2} = 3,425$) at 100 kHz with ± 100 ps jitter, and (c) zone 3,2 at 100 kHz with ± 10 ps jitter.

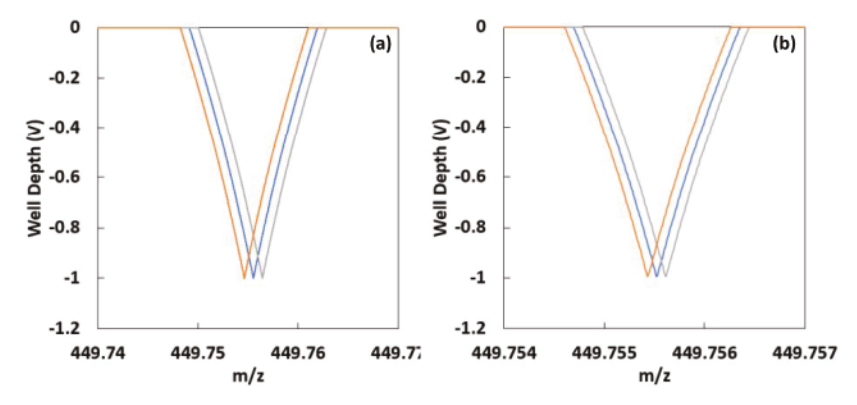


Figure 8. Jitter well spread calculation of (a) zone 4,2 ($RP_{1/2} = 79 \text{ k}$) at 100 kHz with $\pm 10 \text{ ps}$ jitter and (b) zone 5,1 ($RP_{1/2} = 616 \text{ k}$) at 100 kHz with $\pm 1 \text{ ps}$ jitter.

calculated at 99,999.99 (gray), 100,000.00 (blue), and 100,000.01 Hz (orange) with ± 1 ps jitter (0.1 ppm reproducibility) and yield a fractional overlap of 0.77. Note that the well overlaps have similar magnitudes in Figure 8a,b. This result suggests that every order of magnitude increase in resolving power requires an order of magnitude reduction in jitter to achieve the same jitter well overlap. Consequently, to achieve complete overlap as seen in Figures 4a and 7c to optimize resolving power and S/N, both zones 4,2 and 5,1 would require yet another almost order of magnitude decrease in jitter.

PROSPECTS FOR REDUCING COMPARTOR WAVEFORM GENERATION JITTER AND ACCESSING HIGHER ZONES

The zones that are accessible in mass filter operation with good S/N depend on both the acceptance and jitter; both can significantly reduce ion transmission. These two characteristics can be separated by operating the digital linear quadrupole as an ion trap. Ions of any m/z value can be accepted into the quadrupole with a broadband trapping waveform that guarantees minimal ion loss during entry into the quadrupole. Once the ions cool through collisions with a buffer gas, the waveform frequency and duty cycle can be simultaneously switched to a filtering waveform in any stability zone for a user defined number of filtering cycles whereupon the waveform is switched back to a trapping waveform with a deep well to allow the remaining filtered ions to cool and then be subjected to activation or axial ejection into the next device in a hybrid instrument. This trap/filter/eject process eliminates acceptance issues while allowing the influence of jitter to be determined for each accessible zone. Moreover, the agility of the WFG allows the filtering and cooling cycles to be optimized to minimize ion loss during the filtering process.¹¹

Currently, the low voltage WFG provides the largest contribution to waveform jitter because our measurements show no difference between the measured jitter before and after the high voltage pulse. Our results suggest that the slope of the triangular wave that is currently used for comparison-based WFG defines the jitter at this level. Longer waveform periods yield lower slopes during the comparison process and larger jitter. Triangular waves were chosen for comparison because the slope does not change with amplitude, whereas sine waves add more jitter at higher and lower duty cycles because comparisons occur near the peaks and troughs of the sine wave where the slope becomes shallow. According to our

analysis, increasing the slope of the comparison waveform will reduce the jitter. Fortunately, DDS generation is amenable to any periodic waveform and so trapezoidal waveforms can be used with our generation method to reduce jitter. Figure 9

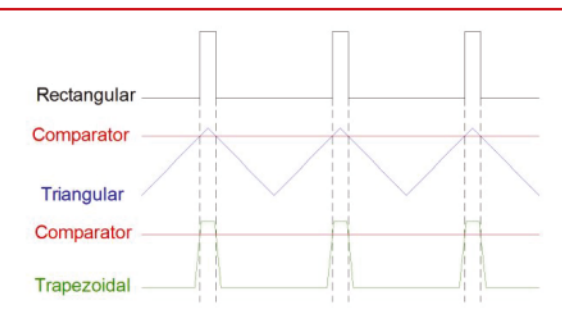


Figure 9. Illustration of comparator-based waveform generation with triangular and trapezoidal waveforms.

illustrates the comparison generation process used with triangular and trapezoidal waves to create the same rectangular wave. When the green trapezoidal wave and the blue triangular wave amplitudes are greater than or equal to the red comparator voltage level, the voltage output of the comparator goes high, and when it is less it goes low to create the rectangular wave output. The advantage is that the slopes of the trapezoidal waves can be programmed with 32 or 48 bits of phase resolution, and so the slopes of the waves can be more than an order of magnitude greater than than the triangular wave at the same frequency and decrease the jitter by the same amount. We project that jitter in the tens of picoseconds range or better can be achieved with trapezoidal waveform comparison. This change in the generation method only requires that the trapezoidal waveforms be programmed into the look up table or the waveform algorythm of the FPGA.

CONCLUSIONS

The ability to access higher stability zones depends largely on the waveform-to-waveform reproducibility as defined by $\Delta T/T$ (the waveform period jitter divided by the period). The Hill equation calculated mass stability pseudopotential wells were used to determine the effect of waveform period jitter. The jitter was used to calculate the frequency range over which the individual waveforms jittered. That frequency range was then used to calculate the jittering extremes of the mass wells. The overlap of the jittering wells was then compared to DMF experiments in higher zones to correlate well overlap with

performance relative to the theory. These calculations were then used to project the jitter requirements needed to access the higher stability zones up to zone 5,1. This work suggests that 10 ps of jitter at 100 kHz can access and utilize all zones up to 4,2. Access to higher stability zones requires a lower jitter.

AUTHOR INFORMATION

Corresponding Author

Peter T. A. Reilly — Washington State University, Department of Chemistry, Pullman, Washington 99164, United States; orcid.org/0000-0001-7679-4511; Email: pete.reilly@wsu.edu

Authors

Sumeet Chakravorty – Washington State University, Department of Chemistry, Pullman, Washington 99164, United States

Fatima Olayemi Obe — Washington State University, Department of Chemistry, Pullman, Washington 99164, United States

Elizabeth Groetsema – Washington State University, Department of Chemistry, Pullman, Washington 99164, United States

Complete contact information is available at: https://pubs.acs.org/10.1021/jasms.2c00293

Notes

The authors declare no competing financial interest.

ACKNOWLEDGMENTS

The authors would like to acknowledge support from the National Science Foundation award #2103645, Phase I funding from the Washington Research Foundation, and technical and material support from SCIEX.

■ REFERENCES

- (1) Konenkov, N. V.; Sudakov, M.; Douglas, D. J. Matrix methods for the calculation of stability diagrams in quadrupole mass spectrometry. J. Am. Soc. Mass Spectrom. 2002, 13 (6), 597-613.
- (2) Brabeck, G. F.; Reilly, P. T. A. Mapping ion stability in digitally driven ion traps and guides. *Int. J. Mass Spectrom.* 2014, 364, 1–8.
- (3) Brabeck, G. F.; Reilly, P. T. Computational Analysis of Quadrupole Mass Filters Employing Nontraditional Waveforms. J. Am. Soc. Mass Spectrom. 2016, 27 (6), 1122–7.
- (4) Reilly, P. T. A.; Brabeck, G. F. Mapping the pseudopotential well for all values of the Mathieu parameter q in digital and sinusoidal ion traps. *Int. J. Mass Spectrom.* 2015, 392, 86–90.
- (5) Huntley, A. P.; Reilly, P. T. A. New tools for theoretical comparison of rectangular and sine wave operation of ion traps, guides and mass filters. *J. Mass Spectrom.* 2020, 55 (12), No. e4661.
- (6) Huntley, A. P.; Reilly, P. T. A. Computational evaluation of a new digital tandem quadrupole mass filter. *J. Mass Spectrom.* 2021, 56 (2), No. e4699.
- (7) Huntley, A. P.; Opacic, B.; Brabeck, G. F.; Reilly, P. T. A. Simulation of instantaneous changes in ion motion with waveform duty cycle. *Int. J. Mass Spectrom.* 2019, 441, 8–13.
- (8) Hoffman, N. M.; Gotlib, Z. P.; Opacic, B.; Clowers, B. H.; Reilly, P. T. A. A comparison based digital waveform generator for high resolution duty cycle. *Review of scientific instruments* 2018, 89 (8), 084101.
- (9) Reilly, P. T. A.; Chakravorty, S.; Bailey, C. F.; Obe, F. O.; Huntley, A. P. Will the Digital Mass Filter Be the Next High-Resolution High-Mass Analyzer? *J. Am. Soc. Mass Spectrom.* 2021, 32 (10), 2615–2620.

- (10) Huntley, A. P.; Reilly, P. T. A. On the relationships between resolution, dimensionless stability, pseudopotential well depth, acceptance, and transmission in mass filters. *J. Mass Spectrom.* 2022, 57 (4), No. e4825.
- (11) Gotlib, Z. P.; Brabeck, G. F.; Reilly, P. T. Methodology and Characterization of Isolation and Preconcentration in a Gas-Filled Digital Linear Ion Guide. *Anal. Chem.* 2017, 89 (7), 4287–4293.